Predicting oil sands viscosity from well logs, NMR logs, and calculated seismic properties

Eric A. Rops and Laurence R. Lines

ABSTRACT

This study is an expansion of the work from last year where it was demonstrated that oil sands viscosity could be predicted directly from standard well logs within 13% error (or 0.72 of one standard deviation) using a real viscosity dataset from Donor Company. This work has been expanded by: normalizing the well logs, using seismic properties calculated from well logs to predict viscosity, adding NMR logs as predictors, improving the viscosity training model, and including reservoir depth as a predictor.

Multi-attribute analysis enables a target attribute (viscosity) to be predicted using other known attributes (the well logs). The top well logs for predicting viscosity were: *resistivity, gamma ray, SP, NMR Total Porosity, NMR Free Porosity, and S-wave sonic*. They successfully predicted viscosity with an average validation error of 69,000cP (or 0.69 of one standard deviation). The top seismic properties for predicting viscosity were: *P-wave velocity* and *P-Impedance*. They predicted viscosity with an average validation error of 94,000cP (or 0.94 of one standard deviation). The well logs modeled more viscosity variations than the calculated seismic properties did, and in most cases including depth as a predictor improved the prediction.

INTRODUCTION

The fluid property with the greatest impact on oil sands productivity and recovery is viscosity (Batzle et al 2006). The more viscous the oil, more energy needs to be injected into the system to reduce the viscosity to allow it to flow. Conventional oil viscosity can range from 1 centipoise (cP) [0.001 Pa*s] which is the viscosity of water, to about 10 cP [0.01 Pa*s]. Viscosity of heavy and extra-heavy oils can range from 10 cP [0.01 Pa*s] to 10,000 cP [10 Pa*s]. The most viscous hydrocarbon, bitumen, is a solid at room temperature and softens readily when heated. Viscosity of bitumen can range from 10,000 cP [10 Pa*s] to more than 1,000,000 cP [1,000 Pa*s] (Alboudwarej et al 2006). Figure 1 shows the logarithmic scale of viscosity subdivided by the grade category of oil, and compares it to the viscosities of typical items found in our kitchen. Figure 1 also illustrates the temperature-dependence of viscosity. Clearly, increasing reservoir temperature decreases the viscosity.

Figure 2 shows core plug measurements from the oil sands about 50 km south-southwest of Fort McMurray, Alberta (Kato et al. 2008). The measurements show that both Vp and Vs decrease with increasing temperature (or decreasing viscosity).
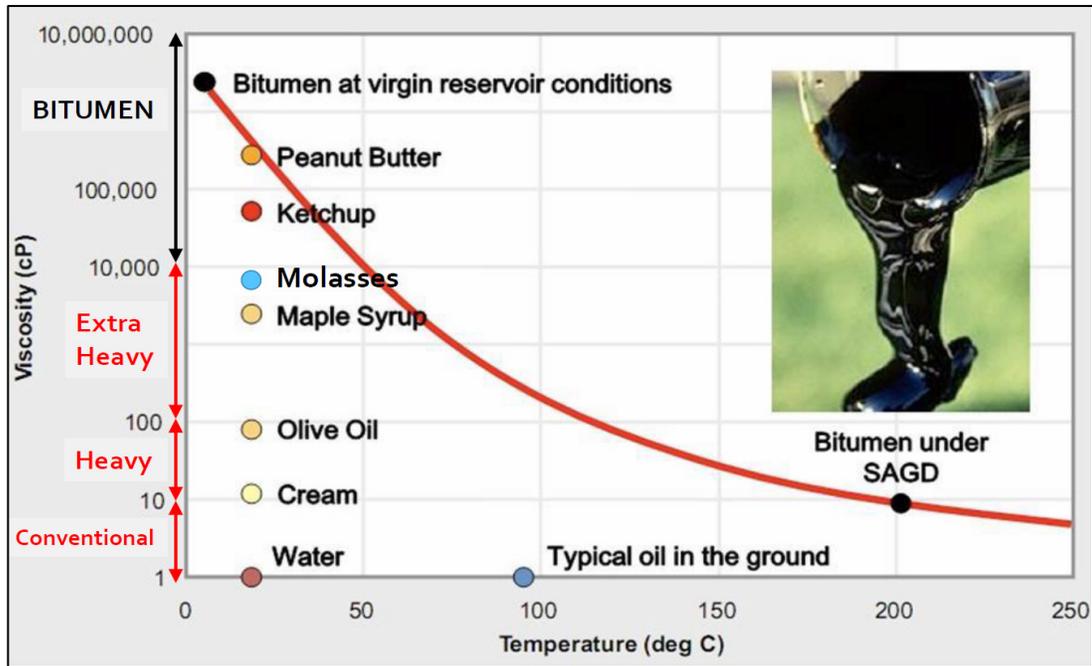
FIG. 1. Oil viscosities by grade category, compared to typical kitchen items. Note that viscosity has a logarithmic scale (ConocoPhillips Oil Sands website).
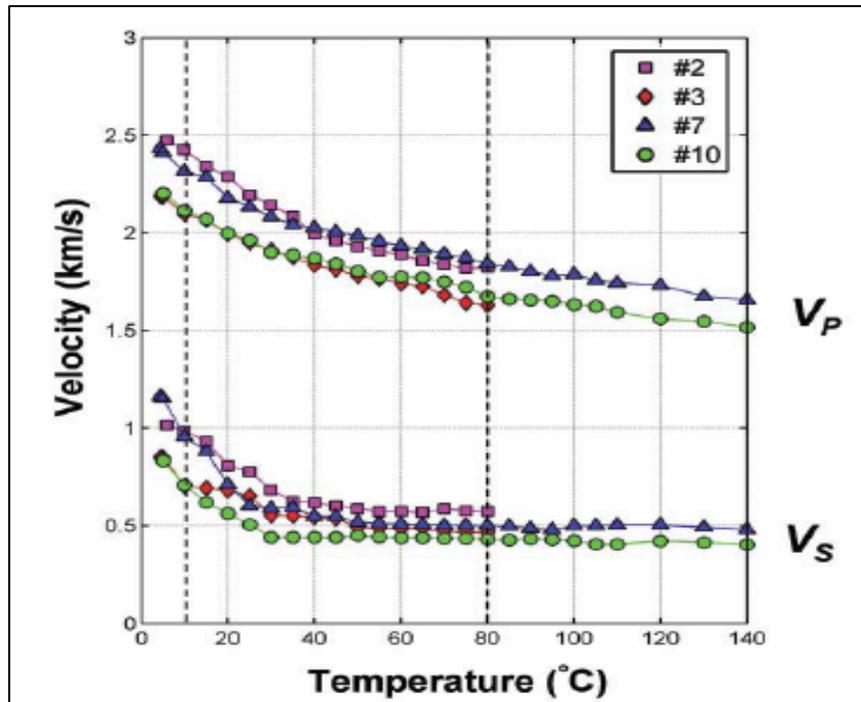
FIG. 2. P-wave and S-wave velocities of oil sands core plugs as a function of temperature at a constant pore pressure of 700 psi and confining pressure 900 psi (Kato et al. 2008).

In addition to its temperature dependence, measurements from Alberta oil sands operations suggest that viscosity also increases with reservoir depth. Figure 3 shows a depth-viscosity plot from ConocoPhillips's Surmont SAGD project, which is located only 10km south of the study area that this report is largely based on. It is not fully understood why bitumen viscosity increases with reservoir depth, but one of the proposed mechanisms is the increased biodegradation near the base of the reservoir due to the bottom-water (ConocoPhillips 2015).
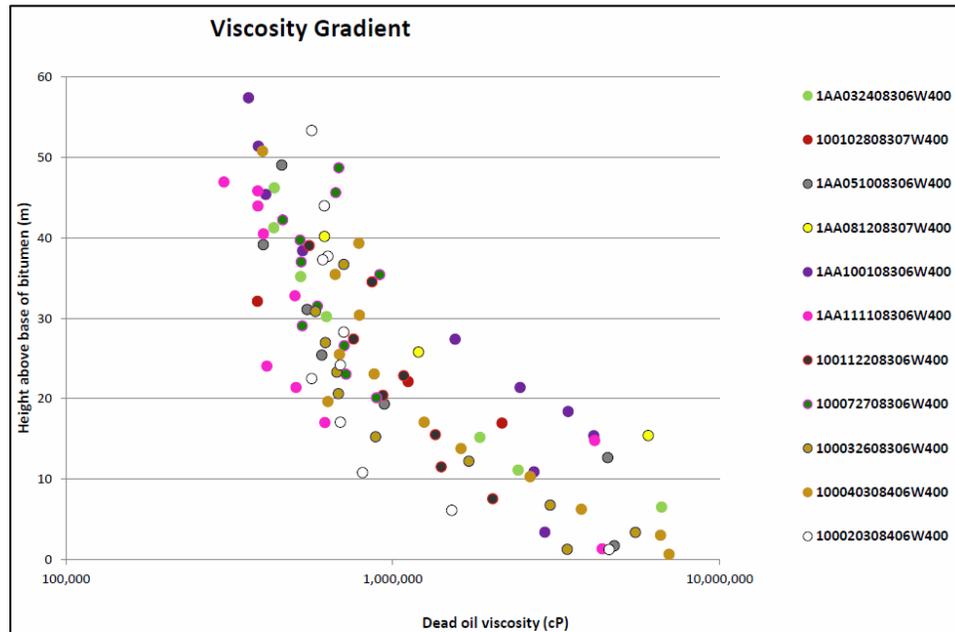
FIG. 3. Core sample viscosity measurements of the McMurray formation from ConocoPhillips's Surmont SAGD oil sands operation, located only 10km south of the study area. This data shows that bitumen viscosity increases with depth in the McMurray formation (ConocoPhillips 2015).

Goal of this study

Donor Company has generously provided viscosity measurements from one of their major oil sands projects, with multiple measurements per well. The goal of this study is to establish a correlation between the measured viscosity values, and *all* of the available well log curves using multi-attribute analysis.

In a previous CREWES report (Rops & Lines 2015b), it was demonstrated that viscosity can be predicted directly from a standard suite of well logs with a prediction error of 13% of the total measured viscosity range.

This report expands on last year's viscosity prediction work by: *normalizing the well logs, using seismic properties calculated from logs, adding in NMR logs, improving the viscosity training model, and including reservoir depth as a predictor.*

THEORY – MULTI ATTRIBUTE ANALYSIS

The theory of multi-attribute analysis is explained in detail in a previous CREWES report from last year (Rops & Lines 2015a). A very brief summary is outlined here, with an additional section about the convolutional operator.

Figure 4 illustrates the basic multi-attribute problem, showing the target log and, in this case, three attribute logs to be used to predict the target attribute (Hampson-Russell 2013).
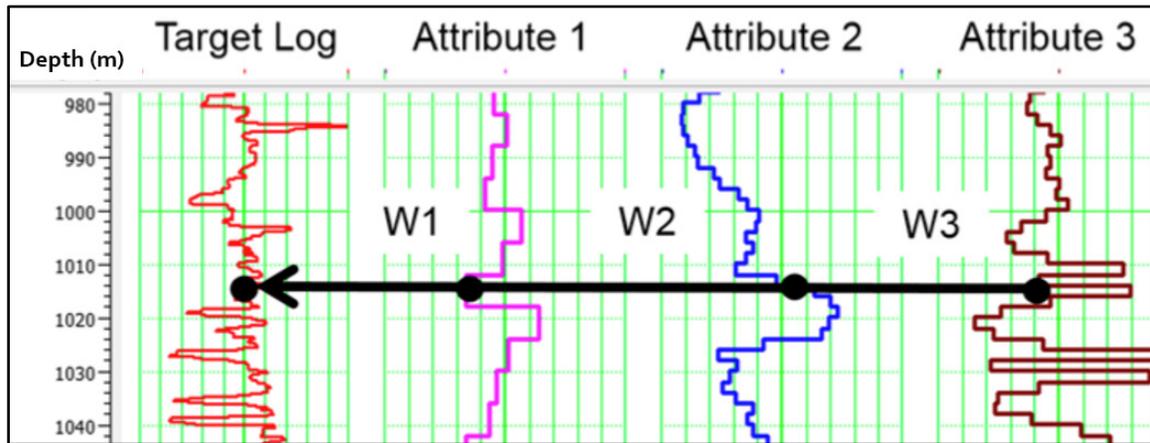
FIG. 4. The basic multi-attribute regression problem showing the target log and in this example, the 3 attributes to be used to predict the target (Hampson-Russell 2013).

To lay out the theory of multi-attribute prediction, let us assume that the target log is P-wave velocity, attribute 1 is bulk density, attribute 2 is gamma-ray, and attribute 3 is resistivity. The goal in this example is to predict P-wave velocity (in the depth domain) from the bulk density, gamma-ray, and resistivity curves.

We can write the fundamental equation for linear prediction as:

$$Vp(z) = w_0 + w_1 D(z) + w_2 G(z) + w_3 R(z) \qquad (1)$$

where $Vp(z)$ is P-wave velocity in m/s, $D(z)$ is bulk density in kg/m^3, and $R(z)$ is resistivity in ohm*m. The regression coefficients $w_1, w_2 \dots w_n$, can be solved for using least squares, and the best predictor attributes can be determined using a statistical method called step-wise regression (Russell 2004). Next, a method called cross-validation is used to determine how *many* attributes should be used to predict the target log (Russell 2004).

Please refer to Rops & Lines (2015a) for a more complete explanation of the theory behind multi-attribute analysis for log prediction.

The convolutional operator

The multi-attribute analysis explained so far correlates each target depth sample with the corresponding sample on each log attribute (as in Figure 4). By using a convolutional operator, each target sample is predicted using a weighted average of a group of samples on each attribute as shown in Figure 5 (Hampson-Russell 2013). For example, if the operator length is set to 5, then each target log sample will be predicted using weighted values of 5 neighboring samples on the attributes.
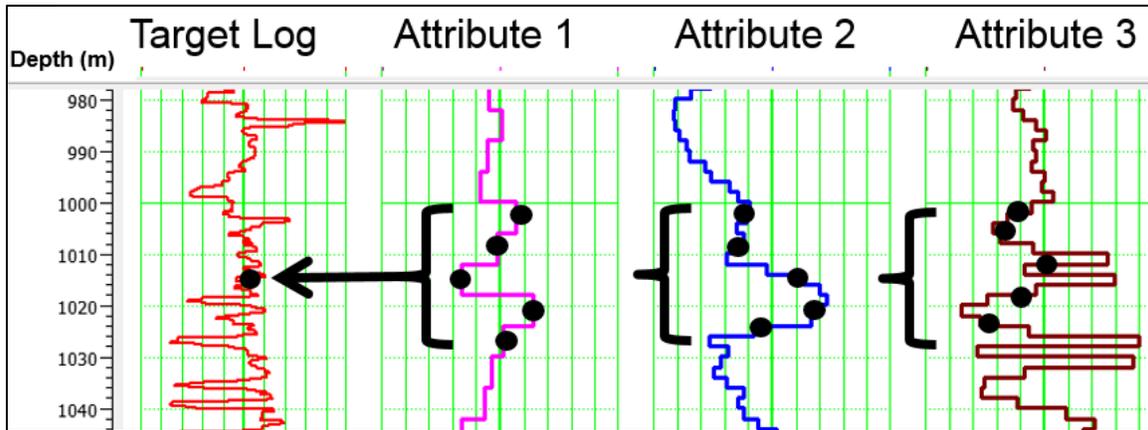
FIG. 5. Illustration of a 5-point convolutional operator, where 5 points for each attribute are averaged for every single point on the target attribute (Hampson-Russell 2013).

Instead of using Equation 1 to predict the target attribute, using a convolutional operator modifies the equation for linear prediction to look like:

$$Vp(z) = w_0 + w_1 * D(z) + w_2 * G(z) + w_3 * R(z) \qquad (2)$$

where "*" represents convolution by an operator (Hampson-Russell 2013).

Using the convolutional operator is like adding more attributes, it will always improve the prediction error, but the validation error may not improve and the danger of over-training is increased (Rops & Lines 2015a). Figure 6 shows a validation error plot where 5 different operator lengths are used to predict P-wave velocity (Hampson-Russell 2013). In this example the validation error is minimized when a 7-point operator is used with 6 attributes, and using a 9-point operator over-trains the data.
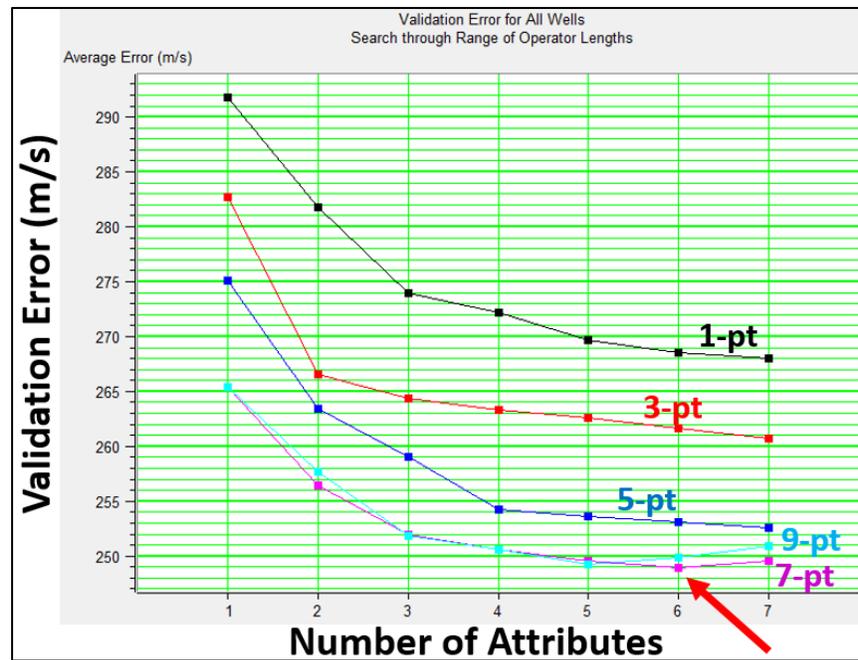
FIG. 6. Validation Error plot for 5 different operator lengths (Hampson-Russell 2013).

PROJECT DATA

The viscosity measurements used for this study were provided by Donor Company from one of their major SAGD (steam-assisted gravity drainage) oil sands projects. Figure 7a shows a regional map of where the project is located. The wells each had cores taken from the McMurray formation. The bitumen was extracted from the cores by a 3rd party laboratory and the kinematic viscosities were measured at 35ºC, 55ºC, and 75ºC. The measurements at 35ºC were used for this study which most closely resembles reservoir conditions. Viscosity was measured at multiple depths, ranging from 2 to 8 depth samples per well. The majority of wells had 3 viscosity measurements.

Figure 7b shows a zoomed-in view of the project location. There are 40 wells in this area with viscosity measurements which have *all* of the well log attributes available in LAS format. Figure 8 shows the distribution of the viscosity measurements. The viscosities (measured at 35ºC) range from 9,000 cP to 550,000 cP, with an average measured viscosity of 121,000 cP, and standard deviation of 100,000cP. Note that the virgin reservoir conditions would be closer to about 10ºC, and the viscosities much higher.

In order to train a multi-attribute relation to predict viscosity from other logs, we need to have viscosity "logs" in the Hampson-Russell Emerge® database. Viscosity logs were manually created for each well by linearly interpolating the viscosities between each measurement point, and nulling the log everywhere outside of the reservoir interval. This is shown in a type well in Figure 9, where the three viscosity measurements are denoted by the red points, and the black curve is the interpolated target viscosity log.

FIG. 7a. Location map of Donor Company's SAGD project (Google Earth®).
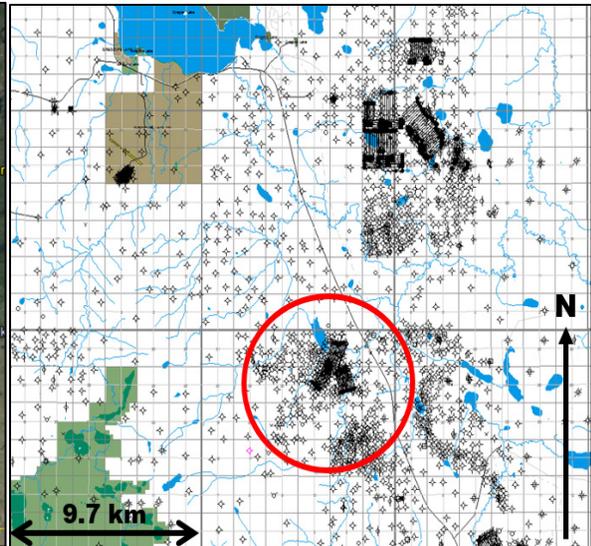
FIG. 7b. Zoomed-in view of the project area. All of the study wells are located within the red circle. Image from geoSCOUT®.
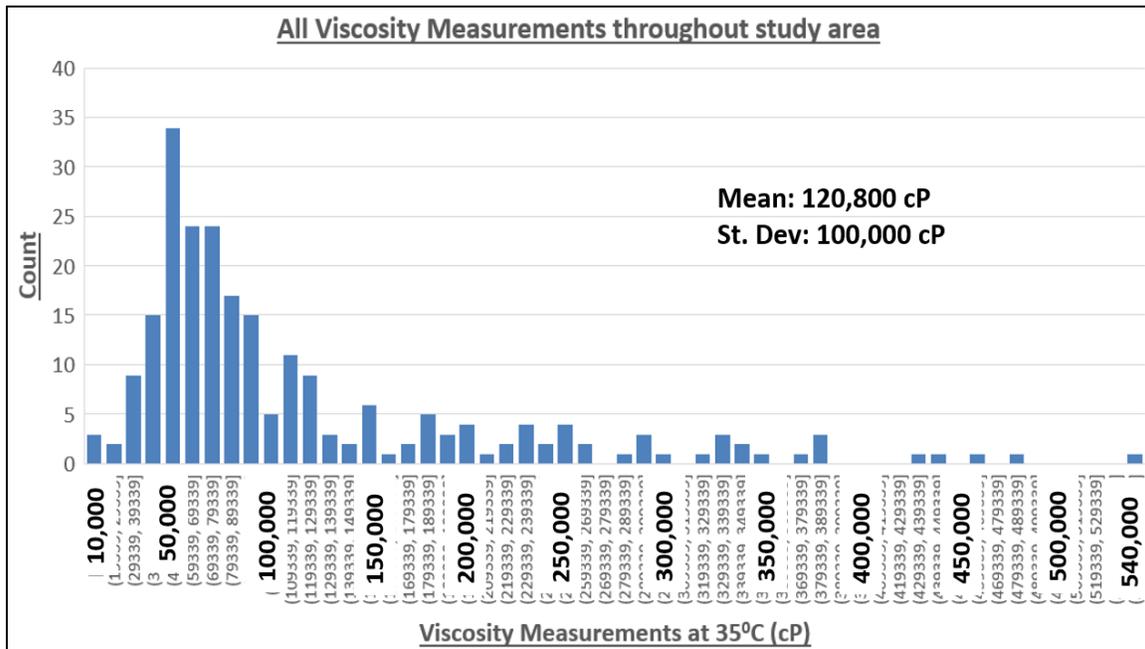
FIG. 8. Distribution of all the laboratory viscosity measurements throughout the study area.
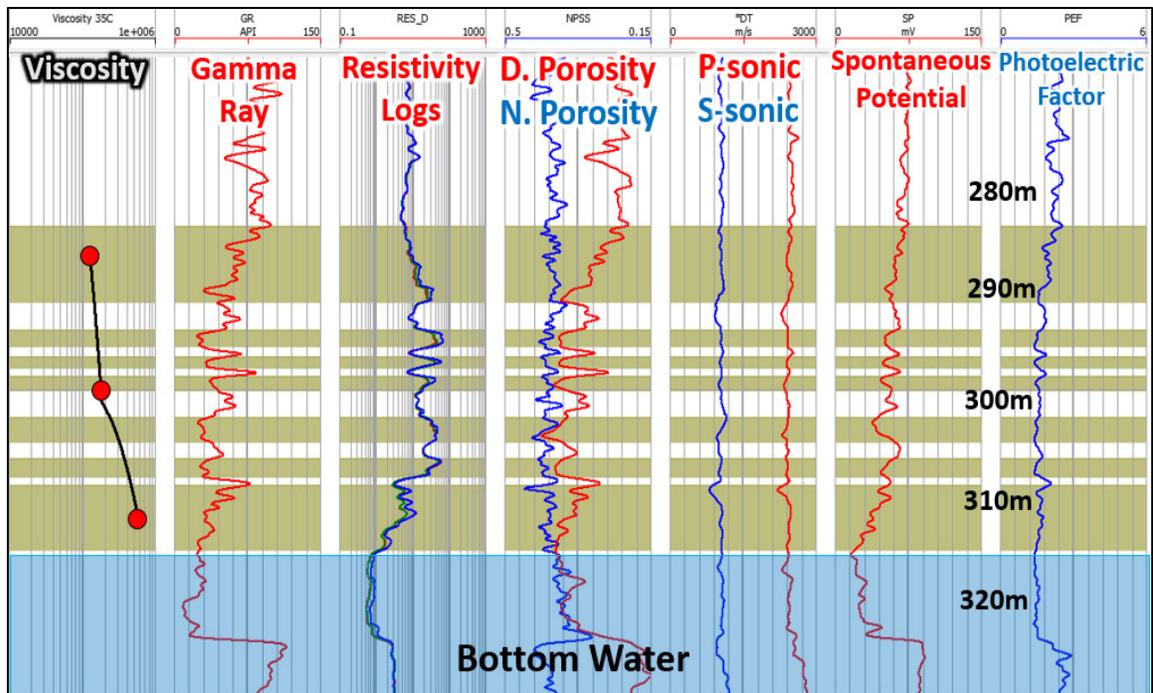
FIG. 9. Type well of the project area. The red dots in the left track are the provided viscosity measurements and the black curve is the interpolated target viscosity log. The viscosity is presented on a logarithmic scale from 10,000 cP to 1,000,000 cP. The gold zones highlight the training intervals (with mud barriers being avoided). There is bottom-water present at the base of the reservoir, based on the low resistivity, high porosity, and high sand content.

The expected trend of increasing viscosity with depth is also apparent. The gold-colored zones highlight the training intervals (ie. reservoir sands). Note that the mud barriers had to be avoided when selecting the training intervals. The low-permeability shale intervals act as barriers and do not contain bitumen, if they were included in the training it would result in highly erroneous viscosity predictions.

Figure 9 also nicely illustrates the presence of bottom-water below the bitumen, which is believed to be a factor causing viscosity to increase with reservoir depth.

WELL LOG NORMALIZATION PROCESS

Well log normalization identifies and removes systematic errors from well log data so that reliable results may be obtained for reservoir evaluation, solving difficult correlation and quantitative problems (Shier 2004). Reasons for tool inaccuracies include varying borehole conditions from well to well, improper wellsite tool calibrations, or using different logging companies in the same area (Shier 2004).

There are a number of methods for normalizing logs in a cluster of wells. For this study the "Big Histogram Method" was used, which adjusts the logs within a zone of interest to have the same average and standard deviation value from well to well. Figure 10 illustrates this concept for the gamma ray logs. The histogram shows the distribution of gamma ray values for all wells from top to base of the gross bitumen interval.
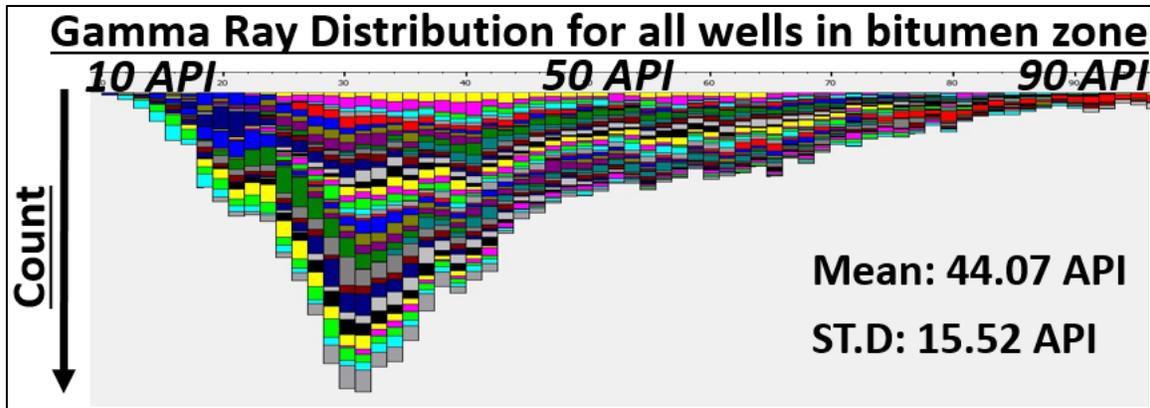
FIG. 10. Distribution of the gamma ray values for all wells from top to base of the gross bitumen interval. Each color represents a different well.
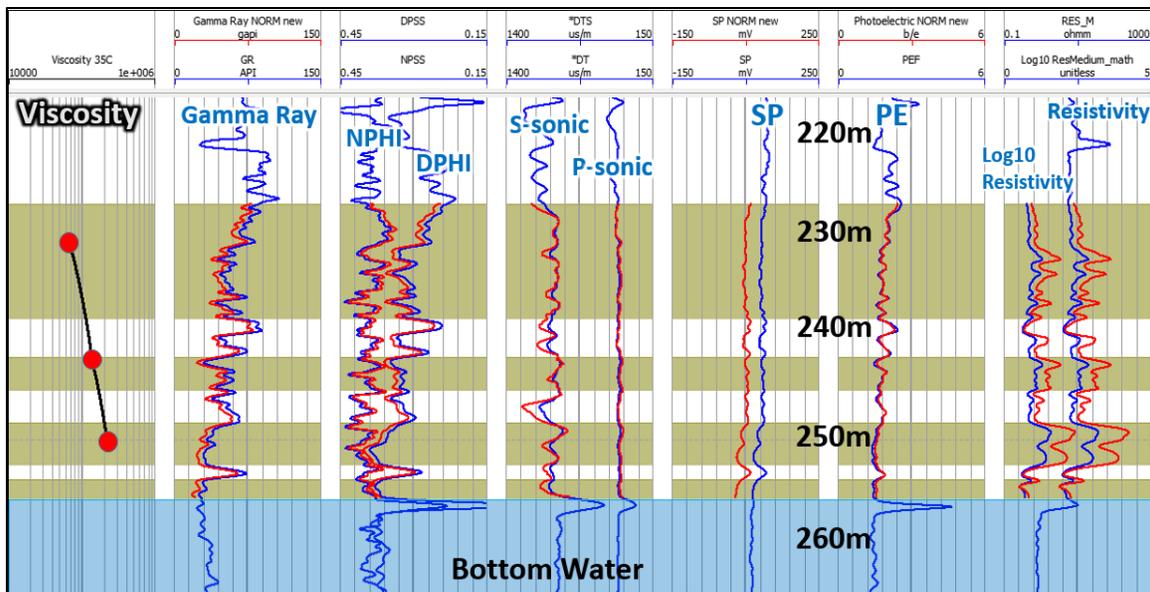
FIG. 11. What the normalized logs look like (red) versus the un-normalized logs (blue). The normalization was focused from top to base of the gross bitumen interval. The gold zones highlight the bitumen intervals.

The gamma ray logs for *each well* were then adjusted so that the average and standard deviation values match the global average (44.07 API and 15.52 API respectively) using the normalization equation at each depth sample:

$$Output(i) = \frac{Log(i) - Average}{StdDev}(DesiredStdDev) + DesiredMean \qquad (3)$$

where *Average* and *StdDev* represent the average and standard deviation values of the log for a specific well, and *DesiredStdDev* and *DesiredMean* represent the global values that each well is to adjusted to match.

Figure 11 shows an example well of how the normalized logs (red) compare to the un-normalized logs (blue). The normalized logs resemble bulk shifted versions of the original

logs to match the global average, with some slight character changes to match the global standard deviation. To normalize the resistivity logs, the *logarithm* of resistivity was normalized and converted back to ohm*m units, since resistivity has a logarithmic scale.

VISCOSITY PREDICTION RESULTS

We will now use the multivariate procedure described in Rops & Lines (2015a) to predict new pseudo-viscosity logs in the project area (using the Hampson-Russell Emerge™ prediction software). The wells having *all* the necessary well logs available in LAS format (40 wells) were used to train the train the relationship between viscosity and the well log attributes. The deep and shallow resistivity logs were omitted since the medium resistivity log was the most consistent, and to avoid duplication of resistivity predictors.

A number of approaches were tried in predicting viscosity, which are outlined in this section.

Predicting linear viscosity versus log10(viscosity) from standard logs

Since viscosity is a logarithmic variable (with respect to temperature), it was attempted to predict both linear viscosity and log10(viscosity). Table 1 and Table 2 show the top predicting attributes for viscosity and log10(viscosity), respectively. Adding more attributes than shown in the tables over-trains the data (ie. the validation error stops decreasing), which is why the tables are truncated and four and three attributes. The log10(viscosity) predictions from Table 2 were converted back to linear space so that the result could be compared against the linear viscosity prediction. This comparison is shown in Figure 12 for 3 example wells, which has the viscosity predictions overtop the true viscosity in the left track. The other tracks contain the well logs used for the viscosity prediction.

	Target (cP)	Attribute	Units	Validation Error (cP)
1	Viscosity	1 / (Medium Resistivity)	1 / (ohmm)	79,100
2	Viscosity	(Gamma Ray)$^{1/2}$	(API)$^{1/2}$	75,900
3	Viscosity	1 / (P-wave sonic)	1 / (μs/m)	73,700
4	Viscosity	ln |Resistivity Separation|	ln|ohmm|	72,000

Table 1. Predicting viscosity directly. Emerge™ prediction attributes with their associated validation errors. All of the well logs from the 40 project wells were used. Note that each row in the list corresponds to a particular multi-attribute transform *and includes all the attributes above it*.

	Target (unitless)	Attribute	Units	Validation Error (unitless)
1	log10(Viscosity)	ln |Medium Resistivity|	ln|ohmm|	0.226
2	log10(Viscosity)	Gamma Ray	API	0.211
3	log10(Viscosity)	1 / (P-wave sonic)	1 / (μs/m)	0.203

Table 2. Predicting log10(viscosity). Emerge™ prediction attributes with their associated validation errors. All of the well logs from the 40 project wells were used. Note that each row in the list corresponds to a particular multi-attribute transform *and includes all the attributes above it*.
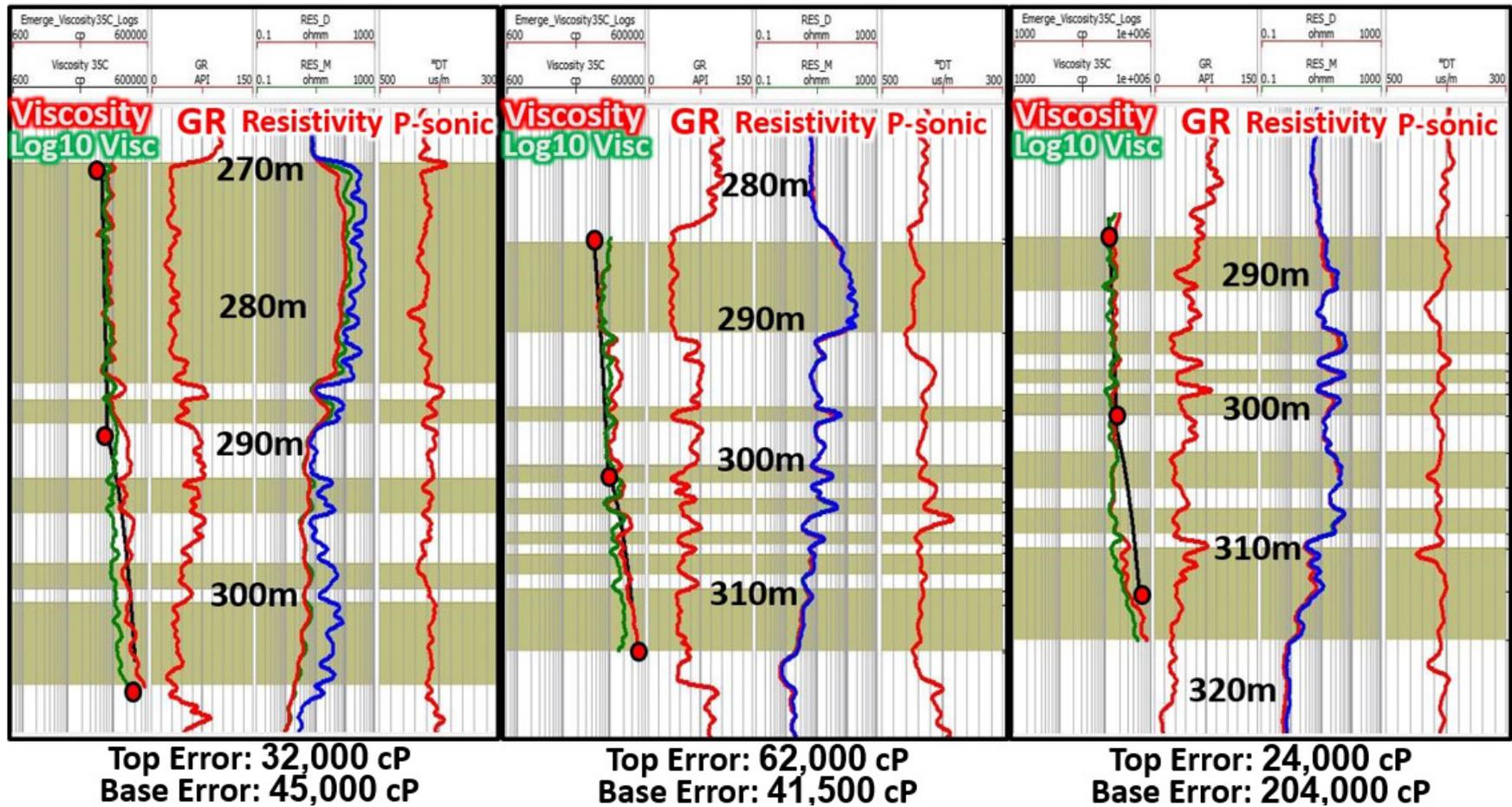
FIG. 12. Predicting viscosity from standard logs. Validation results for three example wells. Each of the 40 wells were systematically left-out and predicted from the remaining 39 wells. The black curves in the viscosity tracks are the true (interpolated) viscosities, the red curves are the predicted linear viscosities and the green curves are the predicted log10(viscosities) converted back to linear space. The logs used to predict viscosity are also plotted. The gold zones highlight the training intervals. Credit: Hampson-Russell Emerge™

Qualitatively it appears the log10(viscosity) prediction is more accurate at the top of the bitumen zone, and less accurate at the base of the bitumen zone.

Figure 13 shows a histogram of the log10(viscosity) errors for all 40 wells converted back to linear space. Quantitatively, the average error is improved from 72,000cP to 49,600cP if we predict log10(viscosity) instead of linear viscosity.
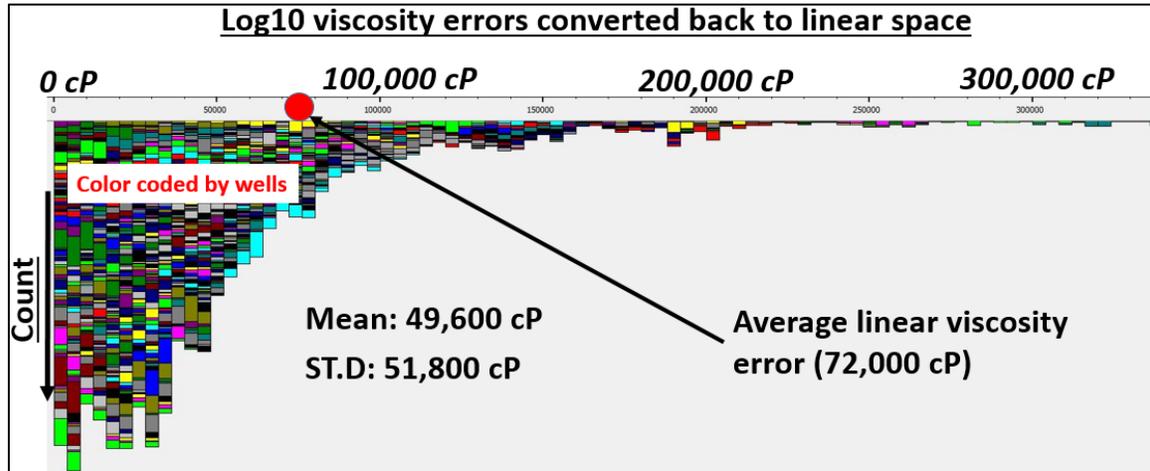
FIG. 13. Log10(viscosity) prediction errors converted back to linear space.

It is speculated that the log10(viscosity) predictions have greater errors in the base reservoir interval because there are less data points constraining the prediction to those high viscosity values. Therefore, the apparent improved prediction error from predicting log10(viscosity) is likely more skewed towards the upper bitumen zone, which has more data points than the lower bitumen zone.

In summary, *Medium Resistivity, Gamma Ray, P-wave Sonic,* and *Resistivity Separation* were the top viscosity predictors with an average validation error of 72,000 cP (13% of total range, or 0.72 of one standard deviation). The un-normalized logs were used since the normalized logs resulted in slightly higher error, which was surprising. A range of operator lengths from 1 to 21 were tried, and they resulted in incremental improvements (a 21-point operator improved the average error from 72,000cP to 70,500cP). These were not significant improvements, so this report focuses on the results from 1-point operators to keep the process straightforward.

Predicting viscosity from calculated seismic properties

It would be immensely valuable for oil sands projects if one day seismic is proven to be able to estimate the viscosity variations within a reservoir. To test this idea in the well logging world, a full suite of seismic properties were calculated from the density, Vp, and Vs logs: *Bulk Modulus, Shear Modulus, P-Impedance, S-Impedance, Vp/Vs, Young's Modulus, Poisson's Ratio, P-Elastic Impedance, PS-Elastic Impedance, and Extended Elastic Impedance.* Figure 14 shows the type well with all the calculated seismic properties which were used to predict the target viscosity (left track). Table 3 shows the top seismic properties for predicting viscosity from Emerge™. The validation error levels off after using five attributes, adding more over-trains the prediction.
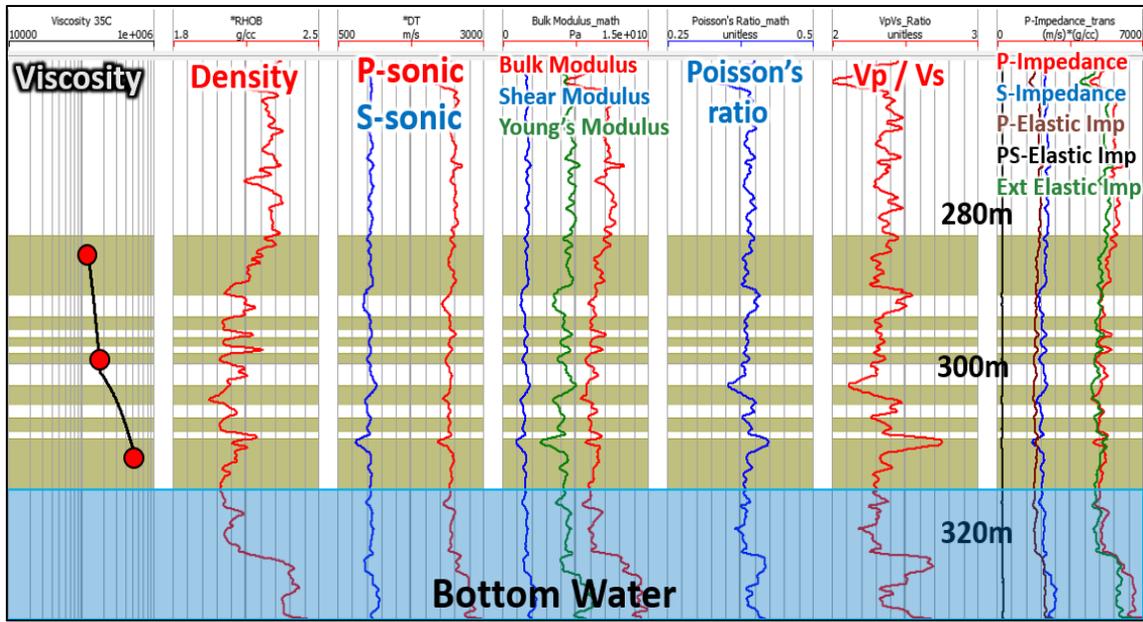
FIG. 14. Type well of the project area with calculated seismic properties. The red dots in the left track are the provided viscosity measurements and the black curve is the interpolated target viscosity log. The viscosity is presented on a logarithmic scale from 10,000 cP to 1,000,000 cP. The gold zones highlight the training intervals (with mud barriers being avoided).

	Target (cP)	Attribute (normalized)	Units	Validation Error (cP)
1	Viscosity	Bulk Modulus	[Pa]	85,800
2	Viscosity	1 / Density	$1 / [kg/m^3]$	85,200
3	Viscosity	1 / (PS-Elastic Impedance)	$[m/s * g/cc]^{-1}$	85,400
4	Viscosity	(Young's Modulus)$^{1/2}$	$[Pa]^{1/2}$	84,000
5	Viscosity	P-Elastic Impedance	[m/s * g/cc]	83,300

Table 3. Predicting viscosity from calculated seismic properties. Emerge™ prediction attributes with their associated validation errors. All of the well logs from the 40 project wells were used. Note that each row in the list corresponds to a particular multi-attribute transform *and includes all the attributes above it*.

Similar to the previous section, these same seismic properties were used to predict the *log10 of viscosity* and converted back to linear space to see if that gets us closer to the measured values. Figure 15 shows the predicted viscosity (red) and log10 of viscosity converted back to linear space (green) overtop the true viscosity in the left track for the three example wells. The other tracks show the seismic properties used for the prediction.

The seismic properties viscosity predictions (Figure 15) are less dynamic than the standard well log viscosity predictions (Figure 12). The seismic properties estimate viscosity reasonably well in the upper reservoir intervals, but greatly underestimate in the bottom reservoir intervals. There is little noticeable difference between the linear and log10 viscosity predictions, however the log10 viscosity prediction is slightly more accurate in the upper intervals, and slightly less accurate in the lower intervals.
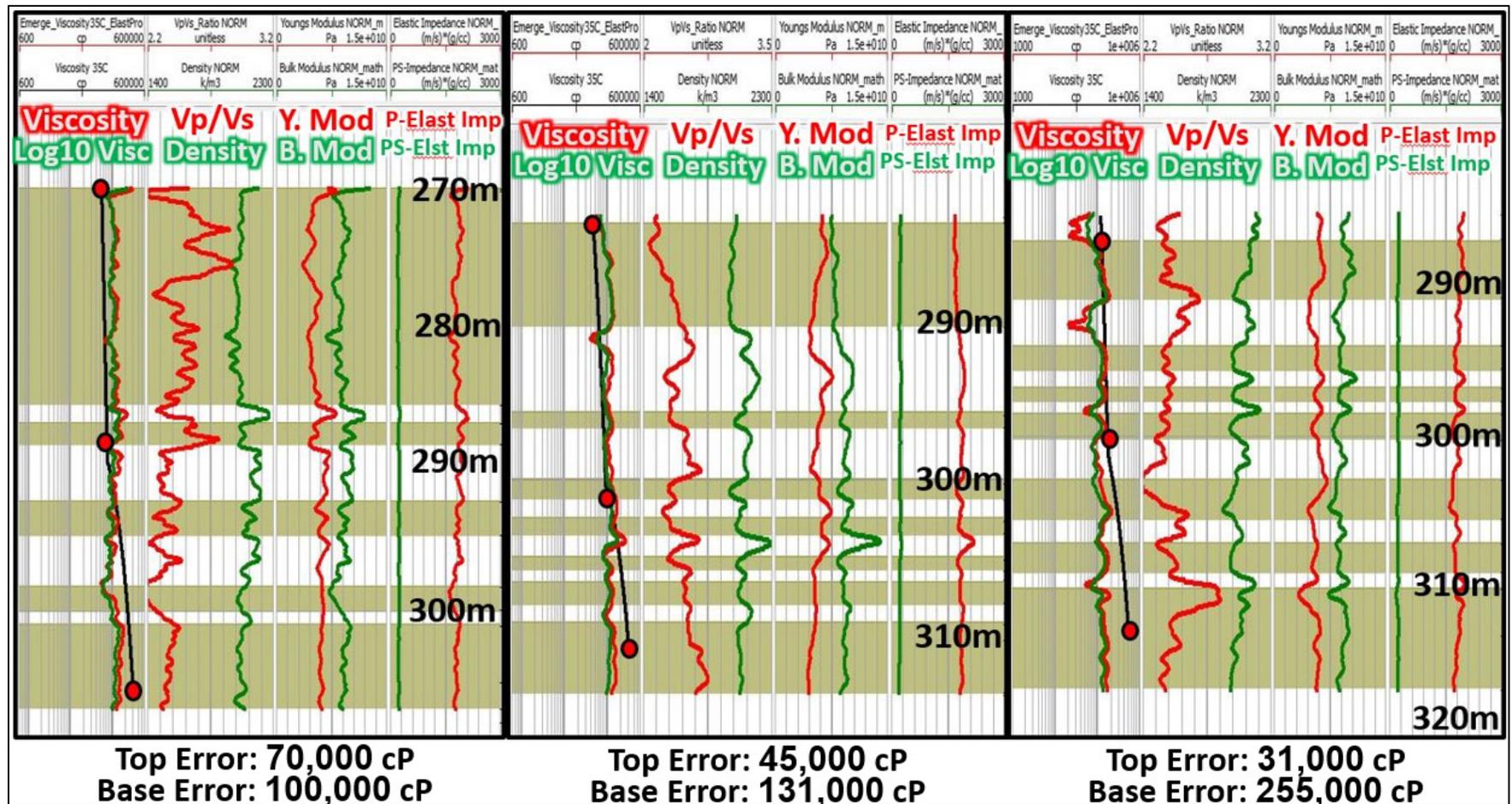
FIG. 15. Predicting viscosity from calculated seismic properties. Validation results for three example wells. Each of the 40 wells were systematically left-out and predicted from the remaining 39 wells. The black curves in the viscosity tracks are the true (interpolated) viscosities, the red curves are the predicted linear viscosities and the green curves are the predicted log10(viscosities) converted back to linear space. The logs used to predict viscosity are also plotted. The gold zones highlight the training intervals. Credit: Hampson-Russell Emerge™.

In summary, *Bulk Modulus, Density, PS-Elastic Impedance, Young's Modulus, and P-Elastic Impedance* were the top viscosity predictors with an average validation error of 83,000 cP (16% of total range, or 0.83 of one standard deviation). The *normalized logs* were used to calculate the seismic properties because they yielded more stable predictions with a lower error than using the un-normalized logs.

Adding NMR logs as viscosity predictors

Unlike conventional logging measurements (ie. acoustic, density, and resistivity), which respond to both the rock matrix and fluid properties and are strongly dependent on mineralogy, NMR-logging measurements respond to the presence of hydrogen protons, which primarily occur in pore fluids. NMR (nuclear magnetic resonance) provides information about the quantities of fluids present, the properties of these fluids, and the *pore size distributions* containing these fluids (Rider & Kennedy 2011).

The NMR measurement is extremely sensitive and complex, who's full explanation is well beyond the scope of this report but can be found in Ellis & Singer (2007). The heart of the measurement involves measuring the characteristic decay time of protons, called the *T_2 relaxation time*, by emitting a sequence of electromagnetic pulses at the correct Larmor frequencies.

Figure 16 shows a typical display of NMR data. The right track shows the T_2 distribution as a function of depth. The left track shows three porosities calculated from the T_2 amplitudes. The rightmost curve is the sum of amplitudes greater than 33μs (ie. free fluid
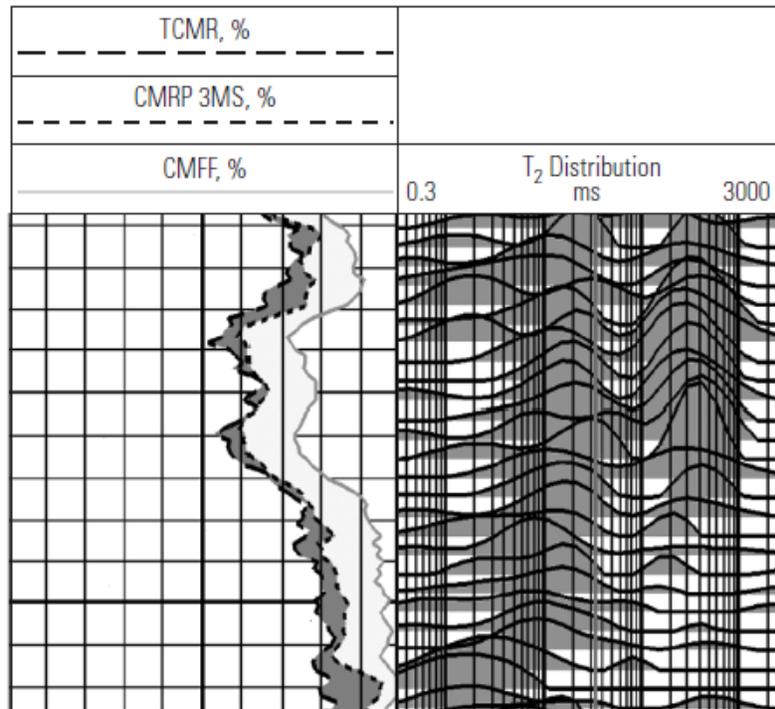
FIG. 16. NMR T_2 distributions as a function of depth are shown in the right track. The left track shows the free-fluid, capillary-bound, and clay-bound porosities calculated from the T_2 amplitudes (Ellis & Singer 2007).

porosity). Between this lower limit and the middle dotted line, shaded in light grey is the additional contribution between 3 and 33 µs (ie. capillary bound fluid). The dark shaded region beyond corresponds to the porosity with T_2 less than 3 µs (ie. clay bound fluid).

In bitumen settings, since the viscosity is extremely large, the T_2 decay times are so low to the point where NMR cannot see the bitumen at all (Ellis & Singer 2007). The simplest way to find bitumen is to compare the density porosity log (which sees all porosity), to the NMR total porosity (which does not see the bitumen), as shown in Figure 17.

Figure 17 shows an example well in the study area, with the NMR total, NMR free, and moveable water porosities plotted. The dark grey area represents the bitumen in the smallest pores and capillaries (not seen by the NMR). The magenta area represents hydrocarbon in small pores and capillaries with poor mobility that the NMR can see. The green represents free (moveable) hydrocarbon in the small to medium pores, and cyan represents free, moveable fluids in the larger pores (Bob Everett, retired Schlumberger petrophysicist, personal communication, November 2016).
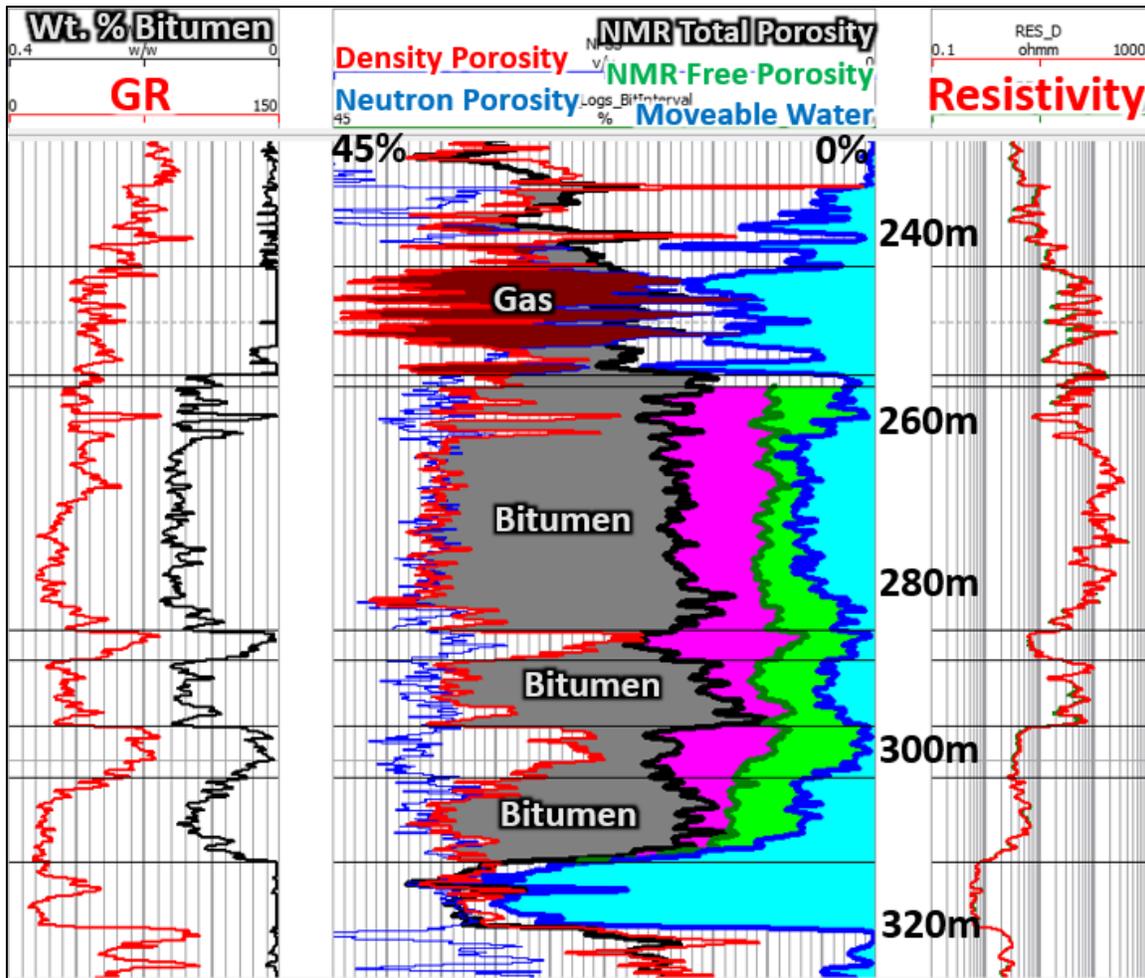
FIG. 17. Oil sands well in the study area with NMR data. The density porosity and NMR total porosity curves overlap above and below the hydrocarbon zones, but separate in the bitumen zones. The grey filled area is bitumen, the filled magenta area is hydrocarbon in small pores and capillaries (seen by NMR), the filled green area is free hydrocarbon in medium pores (seen by NMR), and filled blue is free fluids in the larger pores (seen by NMR).

Note however that these are not true representations of moveable porosities because NMR does not see most of the hydrocarbon porosities in bitumen settings.

It is already known that NMR T_2 distributions can be used to estimate oil viscosity. Sun et. al. (2007) demonstrated that the apparent hydrogen index (HI), which is calculated from the T_2 distribution, shows robust empirical correlations with oil viscosity samples. The goal for this study was to see if combining the NMR data with the standard well logs would improve the data-driven viscosity prediction of this study.

Donor company has generously provided all of their wells in the study area that have NMR data. Unfortunately, *none* of the 25 NMR wells provided have viscosity measurements. Therefore, the 25 NMR wells were used the find the best NMR prediction model from standard well logs. The prediction model was then used to blindly predict the NMR logs in each of the 40 viscosity wells to see if the predicted NMR logs improve the viscosity prediction. Quite an ambitious and possibly laughable task.

Table 4, Table 5, and Table 6 show the Emerge™ top predicting attributes for NMR total porosity, NMR free porosity, and NMR moveable water, respectively. Note that each row corresponds to a particular multi-attribute transform and includes all the rows above it.

	Target (%)	Attribute	Validation Error (%)
1	NMR Total Porosity	1 / (Medium Resistivity)	3.47
2	NMR Total Porosity	(P-wave sonic)$^{1/2}$	3.23
3	NMR Total Porosity	ln |Gamma Ray|	2.96

Table 4. Emerge top predicting attributes for NMR Total Porosity.

	Target (%)	Attribute	Validation Error (%)
1	NMR Free Porosity	1 / (Medium Resistivity)	3.53
2	NMR Free Porosity	(P-wave sonic)^2	3.28
3	NMR Free Porosity	Gamma Ray	3.09

Table 5. Emerge top predicting attributes for NMR Free Porosity.

	Target (%)	Attribute	Validation Error (%)
1	NMR Moveable Water	1 / (Medium Resistivity)	3.45
2	NMR Moveable Water	(Density)$^{1/2}$	3.17
3	NMR Moveable Water	1 / (Neutron Porosity)	2.93
4	NMR Moveable Water	(P-wave sonic)^2	2.79

Table 6. Emerge top predicting attributes for Volume Moveable Water.

Figure 18 shows the predicted NMR porosities plotted overtop of the measured NMR porosities for 2 example wells. The prediction model was trained using all 25 NMR wells from the top to base bitumen interval.

Overall, the raw logs did a slightly better job at predicting the NMR curves than the normalized logs, with an average validation error of 3%. NMR free porosity was the least detailed prediction, but the overall trend was usually still there. Normalizing the NMR logs *before* predicting them made the prediction more unstable, so the results were normalized after they were predicted.
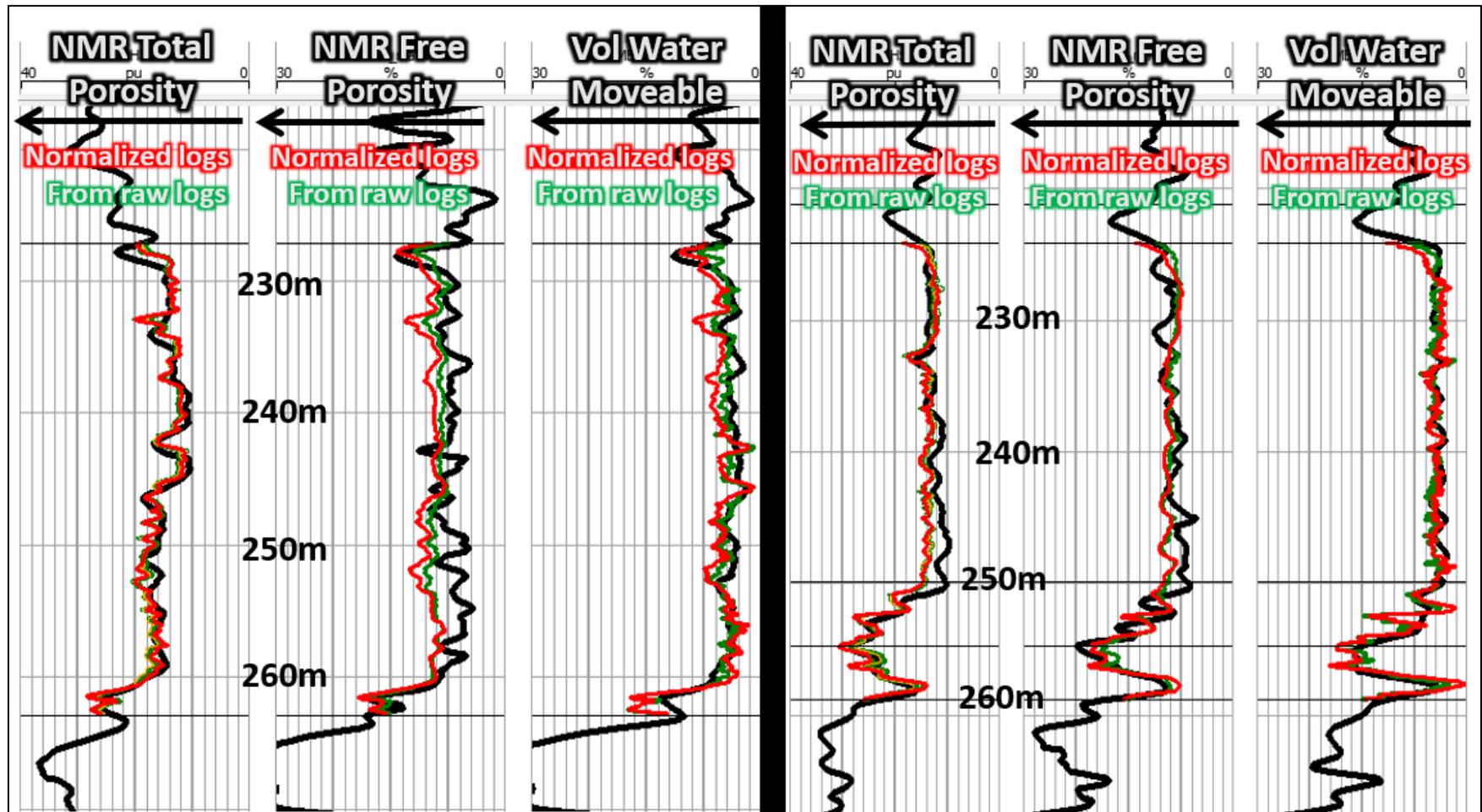
FIG. 18. Predicting NMR porosities from Medium Resistivity, P-wave sonic, Gamma Ray, and Neutron Porosity. Validation results for two example wells are shown. Each of the 25 NMR wells were systematically left-out and predicted from the remaining 24 wells. The black curves are the measured NMR porosities, the red curves are the predicted NMR porosities using *normalized* logs, and the green curves are the predicted NMR porosities using the *un-normalized* (raw) logs. Credit: Hampson-Russell Emerge™

These multi-regression prediction models were then used to blindly predict the NMR porosity logs in each of the 40 viscosity wells. However, before we test if using the predicted NMR logs improves the viscosity prediction, we will first set up an improved viscosity training model.

Improving the viscosity training model

The results so far have involved training the prediction model to best match a target "pseudo viscosity log," which is just a linear interpolation through the actual measured viscosities (shown in Figure 9). This assumes that viscosity varies linearly between each measurement point, which is a significant oversimplification. A more certain method is to train the prediction model at *only the known viscosity measurement depths with the known values.*

Figure 19 shows the new viscosity training model. The left track shows the old target viscosity log in black. The updated target viscosity log is red which is nulled everywhere except around a 100cm window centered at the true measurement depths with the true values. In cases where the measurement depth plotted in a shale interval, it was moved to the nearest clean reservoir interval. Note also that the predicted NMR logs are shown in the porosity track, as described in the previous section.
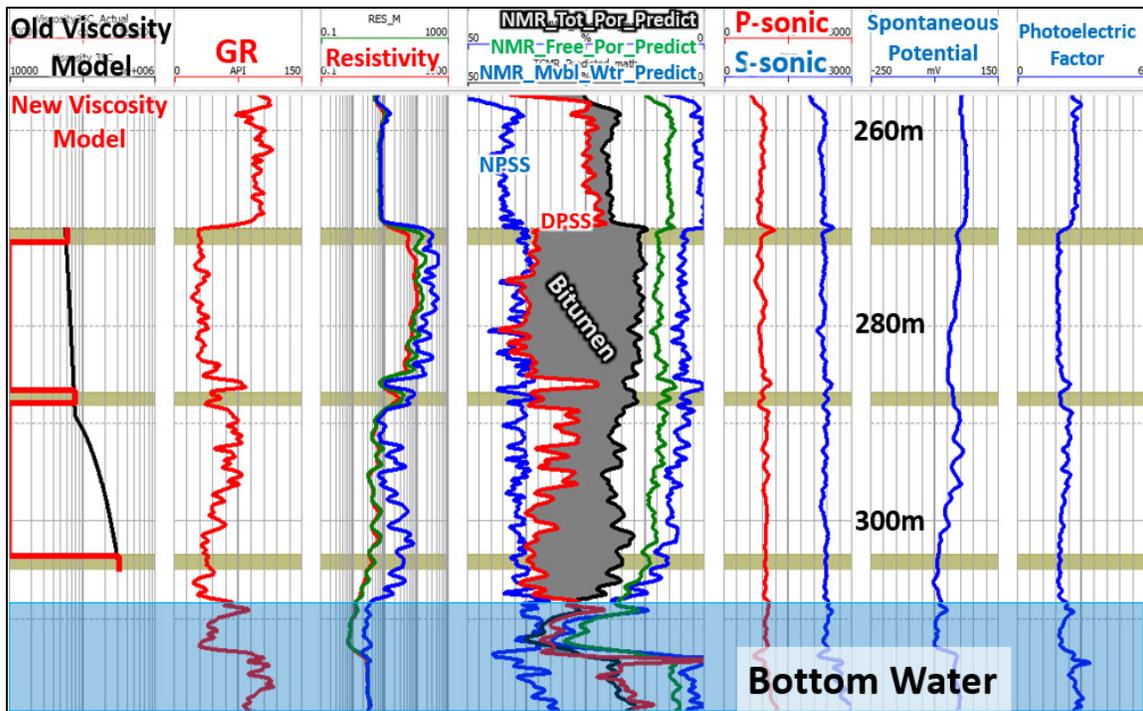
FIG. 19. Updated Viscosity Training Model. In the left track, the black curve is the old (interpolated) target viscosity log. The red curve is the new target viscosity log, with a 1-meter training window centered around the true measurement depth (shown by the gold zones). The viscosity is presented on a logarithmic scale from 10,000 cP to 1,000,000 cP. The predicted NMR porosity logs are also shown, with the shaded grey area indicating the presence of bitumen from the density porosity and NMR total porosity separation.

New viscosity predictions from the updated training model

Table 7 shows the top viscosity predicting attributes from implementing the new training model using standard well logs and the predicted NMR logs. Table 8 shows the top viscosity predicting attributes using calculated seismic properties on the new training model.

	Target (cP)	Attribute (normalized)	Units	Validation Error (cP)
1	Viscosity	1 / (Medium Resistivity)	1 / [ohmm]	84,200
2	Viscosity	ln |Gamma Ray|	ln |API|	77,300
3	Viscosity	1 / (SP)	1 / [mV]	74,800
4	Viscosity	(NMR Total – NMR Free)^2	[decimal]^2	71,600
5	Viscosity	(NMR Total Porosity)^2	[decimal]^2	71,200
6	Viscosity	1 / (S-wave sonic)	1 / [μs/m]	69,500

Table 7. Predicting viscosity from standard logs and predicted NMR logs, with new training model: Emerge™ prediction attributes with their associated validation errors. All of the well logs from the 40 project wells were used. Note that each row in the list corresponds to a particular multi-attribute transform *and includes all the attributes above it*.

	Target (cP)	Attribute (normalized)	Units	Validation Error (cP)
1	Viscosity	1 / (P-wave sonic)	1 / [μs/m]	95,700
2	Viscosity	1 / (P-Impedance)	[m/s * g/cc]$^{-1}$	93,600

Table 8. Predicting viscosity from calculated seismic properties, with new training model: Emerge™ prediction attributes with their associated validation errors. All of the well logs from the 40 project wells were used. Note that each row in the list corresponds to a particular multi-attribute transform *and includes all the attributes above it*.

Figure 20 and Figure 21 show the new viscosity prediction results in two example wells, using the attributes from Table 7 and Table 8. The left side of the figures show the predictions using the well logs, and the right side shows the predictions using calculated seismic properties. The gold zones highlight the reservoir intervals. The magenta colored area is the separation between the predicted NMR Total and NMR Free porosity logs, which came up as the 4th top predictor (Table 7). This separation represents hydrocarbon contained in small pores and capillaries with poor mobility (Bob Everett, retired petrophysicist, personal communication, November 2016).

The well from Figure 20 has bitumen that extends 20m above the shallowest viscosity measurement. Both predictions (using well logs and calculated seismic properties) show good validation agreement with the known viscosities, and they both predict a smooth trend of decreasing viscosity to the top of the bitumen reservoir. The spikes in the predicted viscosity logs occur in non-reservoir intervals, which makes sense because the prediction was only calibrated at the measurement points, which are all in reservoir intervals. There is relatively little difference between the old and new viscosity predictions in this well.

The well from Figure 21 shows more dynamic behavior of the modeled viscosity. On the left side (prediction using well logs), the new viscosity prediction shows more variation than the old prediction. The new model shows a shallow decreasing viscosity profile from 410m to 420m, and two separate profiles of increasing viscosity in two reservoir intervals separated by a more shaley zone (440m to 460m). On the right side, the viscosity prediction from calculated seismic properties shows less variation, and does not see the same trends.
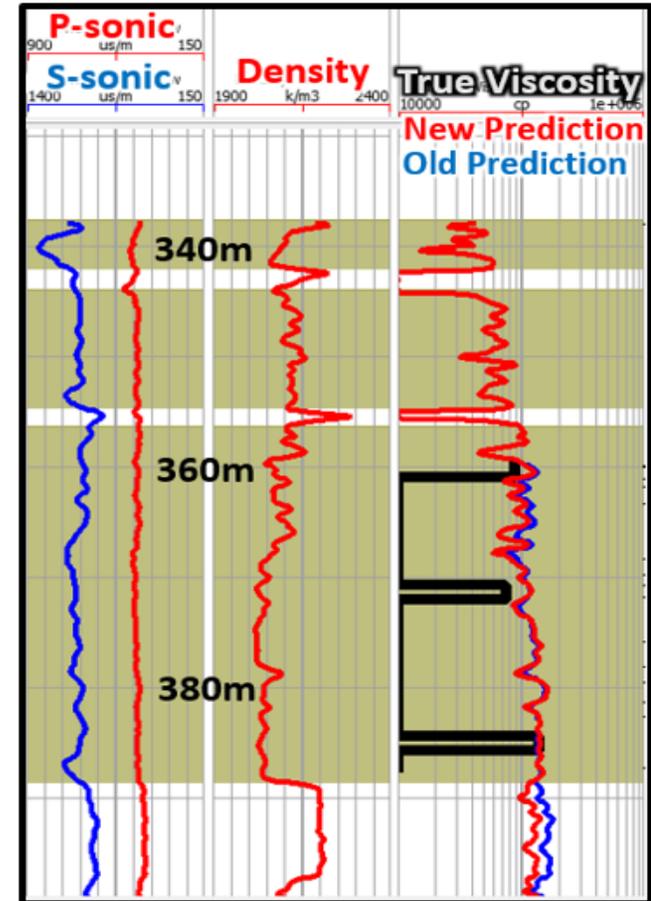
FIG. 20. Predicting viscosity from standard logs and NMR (left side), and calculated seismic properties (right side). Validation results for an example well are shown. The two outermost tracks show the true viscosity measurements (35⁰C) in black, with the new prediction in red overtop the old prediction in blue. The viscosity tracks are presented on logarithmic scales from 10,000cP to 1,000,000cP. The gold zones highlight the bitumen intervals. The magenta colored area is the separation between the predicted NMR Total and NMR Free porosity logs, which represents hydrocarbon contained in small pores and capillaries with poor mobility. Credit: Hampson-Russell Emerge™

FIG. 21. Predicting viscosity from standard logs and NMR (left side), and calculated seismic properties (right side). Validation results for an example well are shown. The two outermost tracks show the true viscosity measurements (35^0C) in black, with the new prediction in red overtop the old prediction in blue. The viscosity tracks are presented on logarithmic scales from 10,000cP to 1,000,000cP. The gold zones highlight the bitumen intervals. The magenta colored area is the separation between the predicted NMR Total and NMR Free porosity logs, which represents hydrocarbon contained in small pores and capillaries with poor mobility. Credit: Hampson-Russell Emerge™

In summary, from implementing the updated viscosity training model (Figure 19) and including predicted NMR logs, the top viscosity predictors were: *Medium Resistivity, Gamma Ray, SP, (NMR Total Porosity – NMR Free Porosity), NMR Total Porosity,* and *S-wave sonic.* The normalized versions of these logs were used because they had lower validation error, and more stable predictions. The average validation error was 69,500 cP (13% of total range, or 0.69 of one standard deviation), an improvement of 2,500cP from using the old, "interpolated viscosity log" training model from Figure 9. The new prediction modelled greater viscosity variation than the old prediction, and more unstable behavior outside of the bitumen intervals.

From implementing the new training model on the calculated seismic properties, the top viscosity predictors were: *P-wave sonic* and *P-Impedance.* The normalized logs were used to calculate the properties because they yielded more stable predictions with a lower error than using un-normalized logs. The average validation error was 93,600 cP (18% of total range, or 0.94 of one standard deviation), which is 10,300cP worse than using the old, "interpolated viscosity log" training model. The new prediction from seismic properties did show slightly more viscosity variation than the old prediction did, but not nearly as much variation as seen by the well logs.

Adding depth as a viscosity predictor

Given the convincing evidence of a depth-viscosity relationship from the ConocoPhillips Surmont project (Figure 3), a similar graph was made for the project area and is shown in Figure 22. A rough logarithmic viscosity trend with depth is apparent.
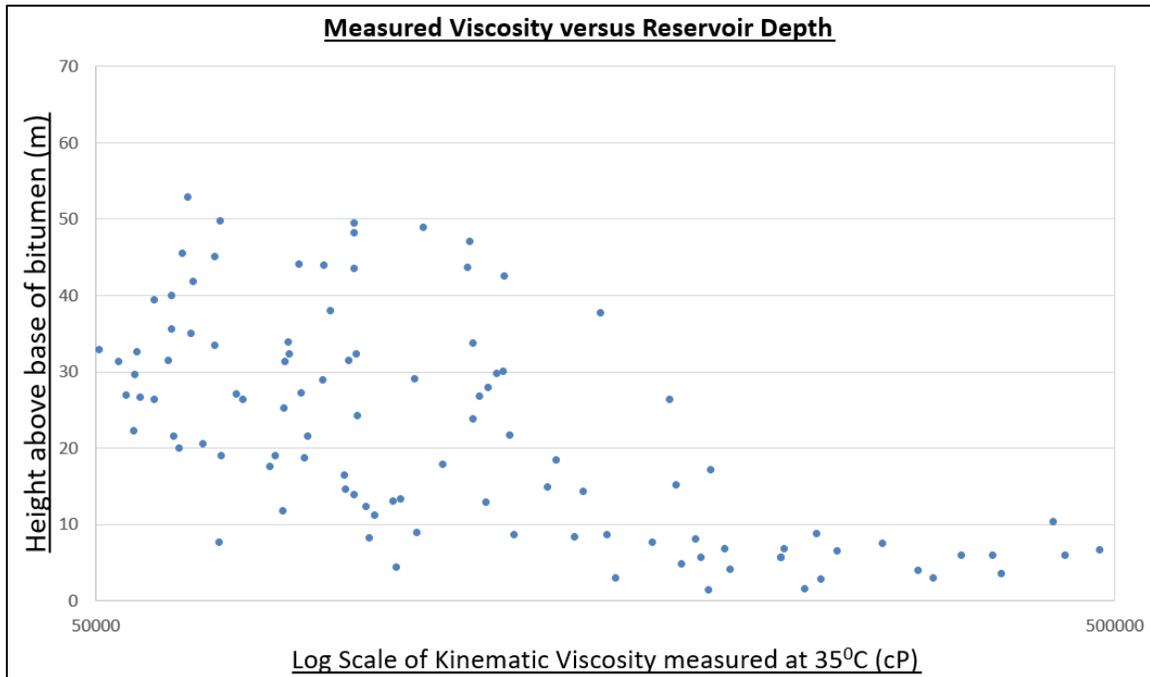
FIG. 22. Reservoir depth vs. viscosity plot. All the viscosity measurements from the 40 study wells are plotted.

Following this line of thinking, base bitumen tops were picked for each of the 40 study wells to generate logs called *height above bitumen base* (depth). The depth logs were then added to the multi-attribute viscosity prediction workflow to see how including depth improves the prediction. Table 9 and Table 10 show to top predicting attributes from well logs and calculated seismic properties, respectively.

	Target (cP)	Attribute (normalized)	Units	Validation Error (cP)
1	Viscosity	ln |HeightAboveBitumenBase|	ln |m|	70,300
2	Viscosity	1 / (SP)	1 / [mV]|	70,000
3	Viscosity	1 / (Log10 Medium Resistivity)	1 / [ohmm]	67,700
4	Viscosity	1 / (Gamma Ray)	1 / [API]	65,900
5	Viscosity	(NMR Free Porosity)^2	[decimal]^2	64,100
6	Viscosity	(NMR Total – NMR Free)$^{1/2}$	[decimal]$^{1/2}$	63,500

Table 9. Predicting viscosity from standard logs, predicted NMR logs, AND depth: Emerge™ prediction attributes with their associated validation errors. All of the well logs from the 40 project wells were used. Note that each row in the list corresponds to a particular multi-attribute transform *and includes all the attributes above it*.

	Target (cP)	Attribute (normalized)	Units	Validation Error (cP)
1	Viscosity	ln |HeightAboveBitumenBase|	ln |m|	70,300
2	Viscosity	1 / (P-wave sonic)	1 / [µs/m]	69,600

Table 10. Predicting viscosity from calculated seismic properties AND depth: Emerge™ prediction attributes with their associated validation errors. All of the well logs from the 40 project wells were used. Note that each row in the list corresponds to a particular multi-attribute transform *and includes all the attributes above it*.

Figure 23 shows how using depth (height above bitumen base) influences the viscosity prediction for three example wells. For each well, the black blocked curves are the true viscosity measurements, and the green logarithmic curves are the predictions using *only depth*. In the left tracks, the viscosity predictions from logs are plotted in blue, and the predictions from logs *and* depth combined are plotted in red. In the right tracks, the viscosity predictions from calculated seismic properties are plotted in blue, and the predictions from seismic *and* depth combined are plotted in red.

For the left and middle wells, depth alone predicts the viscosity trends almost perfectly! Also, combining depth with both the logs and seismic properties improves the prediction instead of using the well logs alone. However, the well on the right has a low measured viscosity near the bitumen base (66,000cP at 440m depth). The depth predictor is not calibrated the predict low viscosities at the reservoir base. As a result, including depth in the prediction overestimates the viscosity at the base, whereas using only the well logs (blue curves) get closer to the true viscosity.

In summary, using depth (height above bitumen base) improved the average validation error from 69,500cP to 63,500cP. In most cases it improves the accuracy of the prediction, however it removes some of the dynamic variations and will always overestimate viscosity if the base of the reservoir has a low viscosity.
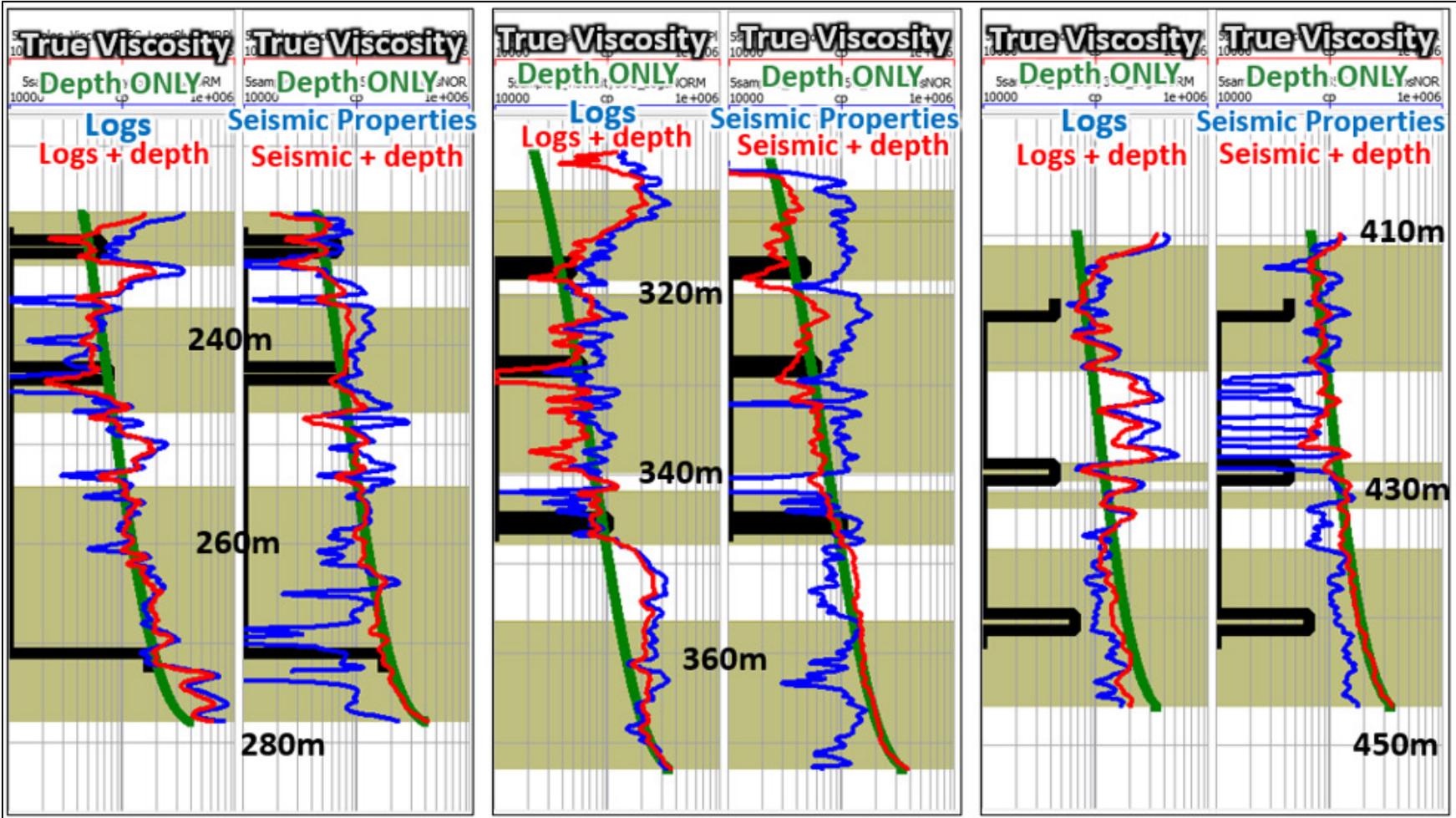
FIG. 23. Influence of depth as a viscosity predictor for three example wells. For each well, the black blocked logs are the true viscosity measurements, and the green logarithmic curves are the predictions using *only depth*. In the left tracks, the viscosity predictions from logs are plotted in blue, and the predictions from logs *and* depth combined are plotted in red. In the right tracks, the viscosity predictions from calculated seismic properties are plotted in blue, and the predictions from seismic *and* depth combined are plotted in red. all viscosity tracks are presented on logarithmic scales from 10,000cP to 1,000,000cP. The gold zones highlight the bitumen intervals. Credit: Hampson-Russell Emerge

Comments about the well logs used to predict viscosity

A number of log types kept re-occurring as viscosity predictors throughout this study: *resistivity, gamma ray, SP, predicted NMR Total Porosity, predicted NMR free porosity, P-wave sonic, and S-wave sonic.*

Resistivity logs are sensitive to changing reservoir fluid types, so it makes sense that resistivity came up as a viscosity predictor, although the exact mechanism is not known. The degree of bitumen saturation in the reservoir ($S_o = 1 - S_w$) might also play a role in predicting viscosity in which case the resistivity of the formation water (R_w), which can change vertically and laterally, would become important. There is also a relationship between Vp and resistivity, first given by Faust (1953):

$$V_p = \gamma \left(Z \frac{R_0}{R_w} \right)^{1/6} \qquad (4)$$

where *Vp* is P-wave velocity in the fluid saturated rock in ft/s, γ is a constant, *Z* is depth in feet, R_0 is the resistivity of 100% water saturated rock in ohm*m, and R_w is the formation water resistivity in ohm*m.

Gamma ray was another common viscosity predictor. The gamma ray log measures the natural radioactivity of the formation, and is commonly used to calculate shale volumes and differentiate between sand units and shale units (Rider & Kennedy 2011). A physical reason why the gamma ray log would be related to viscosity is unclear, perhaps some unique bug deposits or uranium variations?

The SP log routinely came up as a second or third predictor after it was normalized. SP is sensitive to large changes in permeability (Rider & Kennedy 2011), so perhaps it could respond to viscosity variations as well.

It is known that both Vp and Vs decrease with increasing temperature (Figure 2). Since temperature and viscosity are closely related, it follows for Vp and Vs to be sensitive to viscosity variations as well. However, it is surprising that the shear sonic log did not appear more, because viscous bitumen has a non-zero shear modulus compared to conventional hydrocarbons, which the shear sonic should detect. It could be a result of the questionable quality of the shear sonic data in the project area. With better shear sonic data, the viscosity predictions would likely be improved further.

Finally, it is well known that NMR signals can be correlated to viscosity (Sun et. al. 2007). However, none of the viscosity wells in the project had NMR data, so the NMR logs had to be blindly predicted in the viscosity wells by training prediction equations using 25 nearby NMR wells. The fact that the NMR (total – free) porosity separation came up as a predictor is very encouraging. If the viscosity wells had real NMR data, the predictions would almost certainly have been improved further.

CONCLUSIONS

This study demonstrated that multi-attribute analysis of well logs can successfully be used to predict viscosity, given sufficient lab viscosity measurements to train the model. Viscosity estimates within about 70,000cP should now be able to be made on any well in the studied reservoir assuming it has a reliable standard suite of well logs. Note that this model estimates a lab measured viscosity controlled at 35ºC, whereas virgin reservoir viscosities are on the order of millions of cP, at around 10ºC.

Initially, training the model to an interpolated target viscosity log was done. However, it was found that training the prediction model at *only the known viscosity measurement depths with the known value* gives more accurate predictions and reveals more viscosity variations. Table 11 summarizes how all the different predictions compared.

Target Log	Log Set used for prediction	Lowest Validation Error (cP)	# of Attributes
	5 Sample (50 cm) Training Interval (40 training wells)		
	Un-normalized		
Viscosity	Standard Logs	75,700	3
Viscosity	Standard Logs plus NMR	75,000	5
Viscosity	Standard Logs, with NMR plus Depth	63,800	7
Viscosity	Calculated Seismic Properties	97,500	1
	Normalized		
Viscosity	Standard Logs	70,600	5
Viscosity	Standard Logs plus NMR	69,500	6
Viscosity	Standard Logs, with NMR plus Depth	63,500	6
Viscosity	Calculated Seismic Properties	93,600	2
Viscosity	Calculated Seismic Properties plus Depth	69,600	2
Viscosity	*Depth ONLY (Height Above Base Bitumen)*	70,300	1

Table 11. Comparison of viscosity prediction results from using the updated training model.

Normalizing the logs and including predicted NMR logs as viscosity predictors resulted in lower validation errors and more stable predictions.

The calculated seismic properties were less accurate and less dynamic viscosity predictors than the well logs were. However, they still were within 100,000cP most of the time. With improved shear sonic logs, the seismic properties likely would have been more accurate. To extend viscosity prediction into the seismic world, a thick reservoir would be needed for resolution, and very high frequency prestack seismic data to extract out the required elastic properties which would hopefully detect the large viscosity variations throughout the reservoir.

Estimating viscosity ultimately adds value to any heavy oil or oil sands development project because it is used as a main criterion in selecting the recovery method, and it is the *most important parameter* influencing production and development (Batzle et. al. 2006).

ACKNOWLEDGEMENTS

REFERENCES

Alboudwarej, H., Felix, J., Taylor, S., Badry, R., Bremner, C., Brough, B., Skeates, C., Baker, A., Palmer, D., Pattison, K., Beshry, M., Krawchuk, P., Brown, G., Calvo, R., Triana, J., Hathcock, R., Koerner, K., Hughes, T., Kundu, D., Cardenas, J., & West, C. (2006). *Highlighting heavy oil*. Oilfield review, 18(2), 34-53.

Archie, G. E. (1941). *The electrical resistivity log as an aid in determining some reservoir characteristics.* Transactions of the AIME, 146(01), 54-62.

Batzle, M., Hofmann, R., & Han, D. H. (2006). *Heavy oils—seismic properties*. The Leading Edge, 25(6), 750-756.

Beggs, H. D., & Robinson, J. R. (1975). *Estimating the viscosity of crude oil systems*. Journal of Petroleum technology, *27*(09), 1140-1141.

Behura, J., Batzle, M., Hofmann, R., & Dorgan, J. (2007). *Heavy oils: Their shear story*. Geophysics, 72(5), E175-E183.

Bryan, J., Kantzas, A., & Bellehumeur, C. (2005). *Oil-viscosity predictions from low-field NMR measurements.* SPE Reservoir Evaluation & Engineering, *8*(01), 44-52.

Chopra, S., Lines, L. R., Schmitt, D.R., Batzle, M. (2010). *Heavy oils: reservoir characterization and production monitoring*. Society of Exploration Geophysicists.

ConocoPhillips AER Annual Performance Presentation (2015). Subsection 3.1.1 (2f), p.30. Accessed on November 12, 2015. <http://www.aer.ca/documents/oilsands/insitupresentations/2015AthabascaConocoSurmontSAGD94609426.pdf>

De Ghetto, G., Paone, F., & Villa, M. (1995). SPE 30316. *Pressure-Volume-Temperature Correlations for Heavy and Extra Heavy Oils*.

Ellis, D. V., & Singer, J. M. (2007). *Well logging for earth scientists*. Springer Science & Business Media.

Faust, L. Y. (1953). *A velocity function including lithologic variation.* Geophysics, 18(2), 271-288.

Hampson-Russell (2013). *Emerge: Multi-Attribute Analysis* [Course notes].

Han, D. H., Liu, J., & Baztle, M. (2008). *Seismic properties of heavy oils—Measured data*. The Leading Edge, 27(9), 1108-1115.

Kato, A., Onozuka, S., & Nakayama, T. (2008). *Elastic property changes in a bitumen reservoir during steam injection*. The Leading Edge, 27(9), 1124-1131.

Miller, K. A., Nelson, L. A., & Almond, R. M. (2006). *Should you trust your heavy oil viscosity measurement?* Journal of Canadian Petroleum Technology, 45(4), 42-48.

Rider, M., & Kennedy, M. (2011). *The Geological Interpretation of Well Logs. 3rd Edition.* Rider-French Consulting Ltd., Glasgow, Scotland.

Rops, E. A., & Lines, L. R., (2015a). *Predicting heavy oil viscosity from well logs – testing the idea.* CREWES Research Report, Vol 27.

Rops, E. A., & Lines, L. R., (2015b). *Predicting oil sands viscosity from well logs using an industry-provided dataset.* CREWES Research Report, Vol 27.

Russell, B. H. (2004). *The application of multivariate statistics and neural networks to the prediction of reservoir parameters using seismic attributes.* Ph.D. thesis, Department of Geoscience, University of Calgary, Calgary, AB.

Shamsa, A., & Lines, L. (2014). *Effect of oil composition on fluid substitution in heavy oil reservoirs*. Geophysical Prospecting.

Shier, D. E. (2004). *Well log normalization: methods and guidelines.* Petrophysics, 45(03).

Sun, B., Liu, C., Menard, G., Dunn, K. J., & LaTorraca, G. A. (2007, January). *Apparent hydrogen index and its correlation with heavy oil viscosity*. In *48th Annual Logging Symposium*. Society of Petrophysicists and Well-Log Analysts.

Vasheghani, F., & Lines, L. R. (2012). *Estimating heavy oil viscosity from crosswell seismic data.* Journal of Seismic Exploration, 21(3), 247-266.